EVALUATING OPTICAL SYSTEM PERFORMANCE WITH MSC/NASTRAN

Alson E. Hatheway

MSC/NASTRAN User's Conference
March 22-23, 1984
Huntington-Sheraton Hotel
Pasadena, California

Alson E. Hatheway, Incorporated
Consulting Engineers
1041 East Green Street
Pasadena, California 91106
(213) 795-0514

ABSTRACT

It is possible to accurately evaluate the performance of optical components and systems using MSC/NASTRAN. Typical optical parameters are:

Focus, tip and decenter errors
Surface figure changes
Image quality
Wave front quality
Boresight stability
Line of sight control

This paper discussed modeling techniques for evaluating two of these parameters, 1) Boresight stability and 2) Surface figure changes. The paper will be highlighted with examples drawn from recent practice which show the numerical and visual evaluation of these parameters.

4033/AEH.

INTRODUCTION

AEH assists clients in the development of complex optical systems. These systems are expected to operate in hostile environments ranging from below the sea's surface to outer space. AEH has found MSC/NASTRAN a valuable tool in evaluating the optical performance of systems deformed by environmental loads. Optical parameters may be coded in MSC/NASTRAN because the underlying equations of optics are linear. The use of extra GRID points and multi-point constraint (MPC) cards is sufficient to make the optical parameters dependent upon the structural displacement vector. A wide variety of optical parameters may be evaluated using MSC/NASTRAN. Examples in geometric optics and wave optics are shown below.

GEOMETRIC OPTICS (Ray Tracing)

The degrees of freedom available at two GRID points uniquely define the attributes of an optical ray by giving its position of origin in space (GRID A) and its angles of propagation through space (from GRID A to GRID B). Furthermore, one can make the motion of ray GRID points (A and B) dependent upon the motion of structural GRID points and the laws of optics by using Multipoint Constraint (MPC) cards.

For the reflective case (Figure 1), the angle of incidence equals the angle of reflection (the law of reflection) and the change in the angle of reflection equals twice the angular change of the mirror surface. The MPC relationship can be formulated as follows:

$$dr=-di+2ds.$$

Or, if the ray from GRID 1 is fixed in space,

$$dr=2ds.$$

Reformatted for an MPC card and using the notation of Figure 1,

$$d(2)-2d(1000)=0,$$

and,

MPC	SID	2	6	1.0	1000	6	-2.0		

This card defines the angular relationship of the reflected ray departing from GRID 2 based upon the angular change of the structure at GRID 1000. Similar relationships may be written for the other five degrees of freedom of the "ray" GRID 2, so that the complete description of the ray departing GRID 2 is calculated in MSC/NASTRAN.

For the refractive case (Figure 2), a similar relationship exists, but it includes the index of refraction and the sine of the angles (Snell's Law). Assuming the ray from GRID 1 is fixed in space and noting that di=ds,

$$(n_i\cos(i))ds=(n_r\cos(r))dr,$$

or,

$$dr=(n_i/n_r)(\cos(i)/\cos(r))ds.$$

Reformatting for an MPC card and using the notation of Figure 2,

$$d(2)-(n_i/n_r)(\cos(i)/\cos(r))d(1000)=0,$$

and,

MPC	SID	2	6	1.0	1000	6	$(n_r/n_i)(\cos(r)/\cos(i))$	

This card defines the angular relationship of the refracted ray departing GRID 2 based upon the angular change at GRID 1000. Similar relationships may again be written for the other five degrees of freedom at GRID 2 so that the complete description of the ray departing GRID 2 is again calculated in MSC/NASTRAN.

The analyst should recognize that an attribute of a departing ray may be dependant upon more than one attribute of either the incoming ray or the point of incidence. Since the MPC format may extend to more than one card, the analyst may accomodate as many attributes as desired for an accurate solution.

Ray tracing can be added to a model by adding GRID points to the structure which define the ray intercept points for the undeformed structure and then adding extra GRID points (to be controlled by MPC cards) at each ray intercept point. The extra GRID points are interconnected with PLOTEL cards if ray plotting is desired and the MPC cards are prepared in accordance with the optical laws to control the deformed position of the extra GRID points. As an example of ray tracing, consider the afocal cassegrain telescope shown in Figure 3. In this case a paraxial ray (quasi-chief ray) is plotted from object space to primary mirror to secondary mirror to image space. Since this telescope was boresighted with other instruments, we were interested to know the degree of loss of boresight under various operating environments. The quasi-

chief ray is plotted by PLOTELs which are controlled by MPCs according to the above equations. Figure 4 shows the mounting flange deformed by .005 inches as if by a grain of sand trapped in the joint. The listing (Figure 5) shows the angular deviation of the quasi-chief ray in object space (.399 miliradians); this is equivalent to the shift in bore sight of the instrument caused by the deformation of the flange. Since the requested displacement coordinates are in the basic coordinate system, the total bore sight shift is the vector sum of R1 and R2 in the listing. Visual inspection of Figures 3 and 4 disclose the deflected path of the quasi-chief ray.

WAVE OPTICS (INTERFEROMETRY)

Interference fringes are generated in optical systems by the constructive and destructive interference of two coherent bundles of light. The most familiar form of interference is Newton's rings as seen between two glass plates with a small air space between. If the illumination is monochromatic, the pattern is stronger and the rings are more distinct. These rings are used by optical engineers to describe how well an optical surface conforms to their desired shape. In general, because the ring patterns may be an irregular shape, the phenomenon is called a fringe pattern. A surface may be allowed to deviate from a specified surface by a limited number of fringes for a given wave length of illumination. Test plate fringe patterns are illustrated in Figure 6.

The fringes are formed as the air space varies by 1/2 wave length between the surfaces. So, for a fixed optical surface (anchored to avoid whole body motions), the fringe pattern may be derived from an MSC/NASTRAN structural analysis by requesting a contour plot of the optical surface and specifying plot intervals equal to 1/2 the wave length of illumination.

Optical elements mounted in systems usually undergo whole body motions which are much larger than the surface deformation. In this case, the analyst has to model a test plate made of rigid elements to overlay the undeformed optical surface. The test plate is then attached to the optical surface using multi-point constraints (MPCs). Additional MPCs are added to calculate the air space between the test plate and the deformed optical surface and these MPCs are used to deform a third surface to agree with the air space over the optical surface. This third surface (the plot surface) is the one which is contour plotted to yield the interference fringe pattern. The elements of the plot surface are used only to interpolate between the GRID point deflections so that shell and material properties should be selected to minimize the influence of these elements on the rest of the structure, i.e., thin, massless, and soft material.

Let's use the same afocal telescope (Figure 3) to illustrate the above procedure and show the results. From Figure 4, we can observe the whole body motion of the primary mirror because the plotting surface elements were overlayed directly on the mirror surface and MPC'd to have very small motions. The whole body motion represents a tip of about .49 miliradians, which involves axial translations of from $+7.6 \times 10^{-4}$ to -1.2×10^{-3} inches. Clearly a simple contour plot of the primary mirror surface would be dominated by this whole body motion, making the surface figure

unobservable. However, by following the strategy described above, it is possible to remove the whole body motion and observe the underlying change in surface figure.

Figure 7 is a contour plot of the primary mirror plot surface, taking the default of ten equal contours for the full range of deflection. The tabular data is transcribed from the plot module in the MSC/NASTRAN listing. The total range of surface change is from -12.1 microinches to +5.61 microinches. The importance of the above procedure can now be appreciated; we have been able to remove the whole body motion of the optical element in order to disclose surface figure changes which are two orders of magnitude smaller.

In order to interpret the surface figure changes in quantities which are more easily understood by optical engineers, the contour plot of Figure 7 can be replotted with intervals equal to 1/2 wave length of a convenient illumination source. Figure 8 is such a plot. Helium-neon laser illumination has been selected (wave length equals 633 manometers) so that the contour intervals are 12.5 microinches (317 manometers). The optics engineer can immediately appreciate the surface figure changes described in Figure 8, because the results are presented in the form of standard production test fringe patterns with identical interpretation.

Another load case is shown in Figure 9, which shows the surface figure change caused when the telescope is accelerated at 100g along its axis. In this case, the figure change is very large, about 20 fringes in helium-neon light. Clearly this could represent serious deterioration of the optical performance of the telescope. The test facility to uncover this kind of problem would be very large and expensive (the telescope, illuminator, and recording system all swinging on the arm of a centrifuge), however, MSC/NASTRAN can predict these results with relative ease.

CONCLUSION

MSC/NASTRAN can be a very powerful tool in evaluating optical performance of components and systems. The phenomena of geometric optics and wave optics are based upon linear equations and modeling strategies can include optical computations in the MSC/NASTRAN runs. All of this analysis may be done without ALTERs, DMAP statements, or post-processor routines.

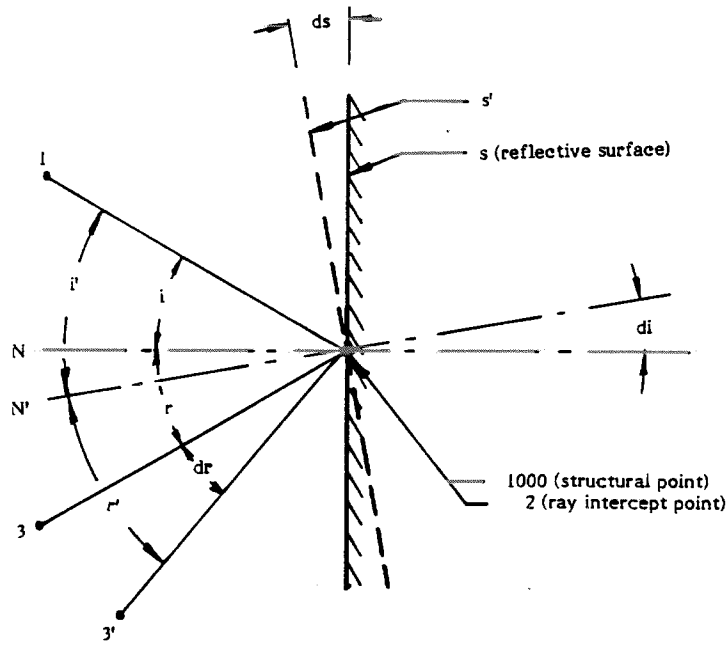

r=-i (fixed surface)
r=-i+2ds (moving surface)
dr=-di+2ds (differential form)

Figure 1. The Law of Reflection.

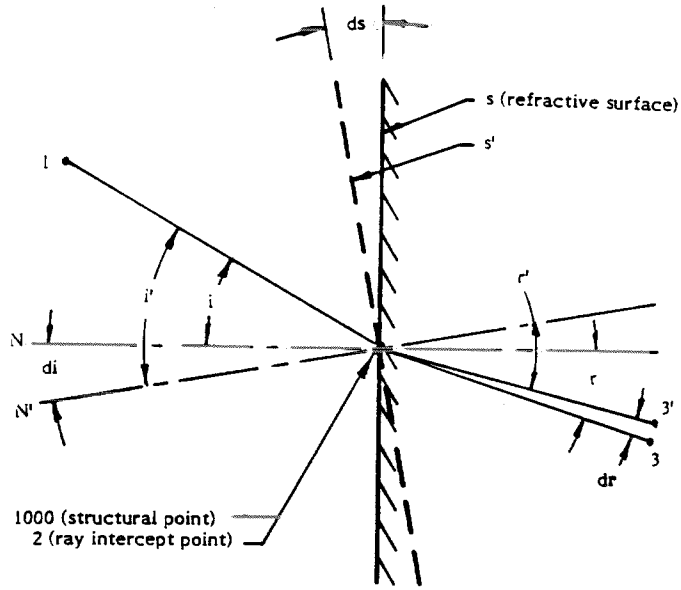

$\sin(i)/\sin(r)=n_r/n_i$ (Snell's Law)

$(n_i\cos(i))di=(n_r\cos(r))dr$ (differential form)

Figure 2. The Law of Refraction.

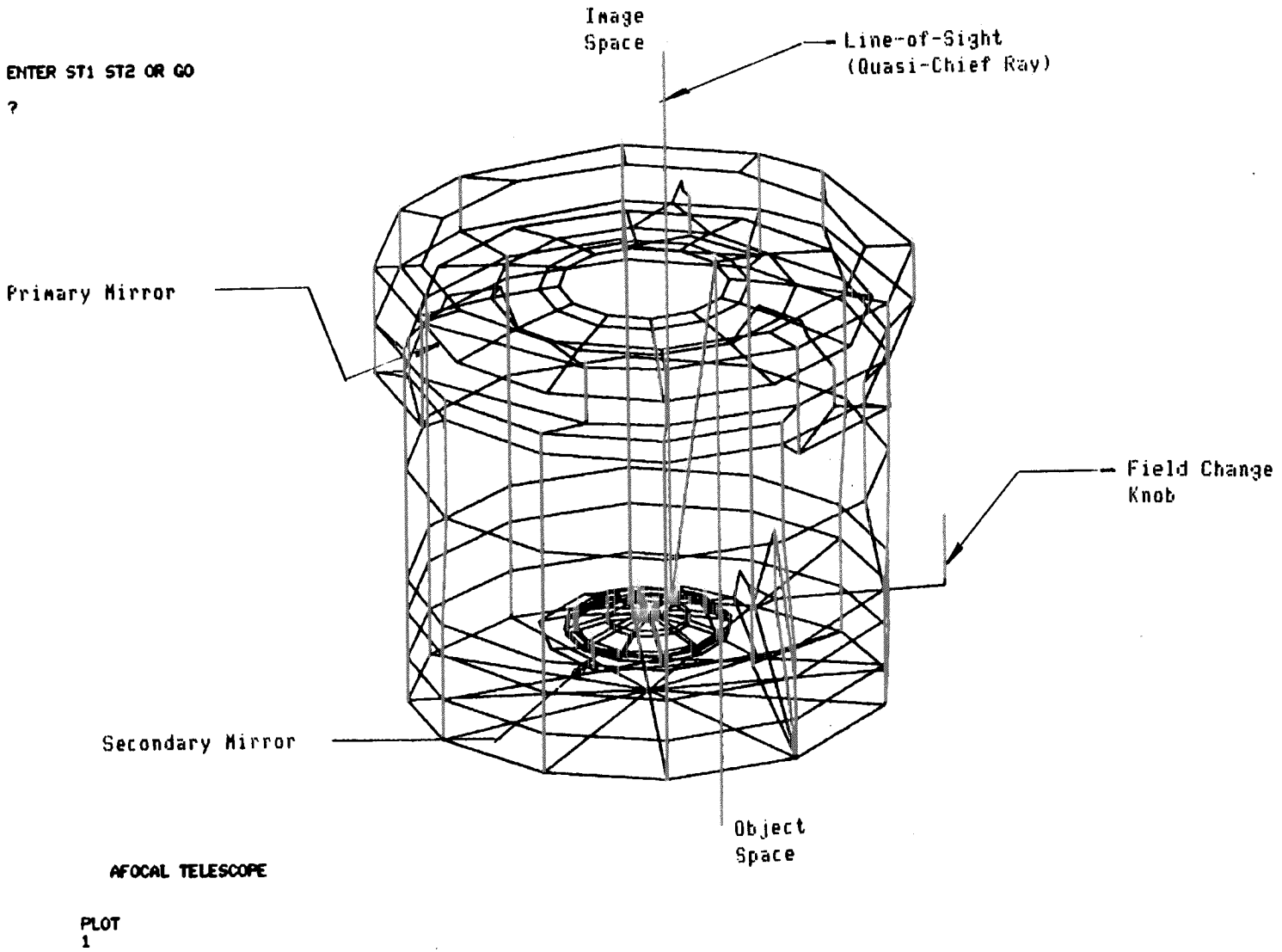

Figure 3. Afocal Telescope Attachement.

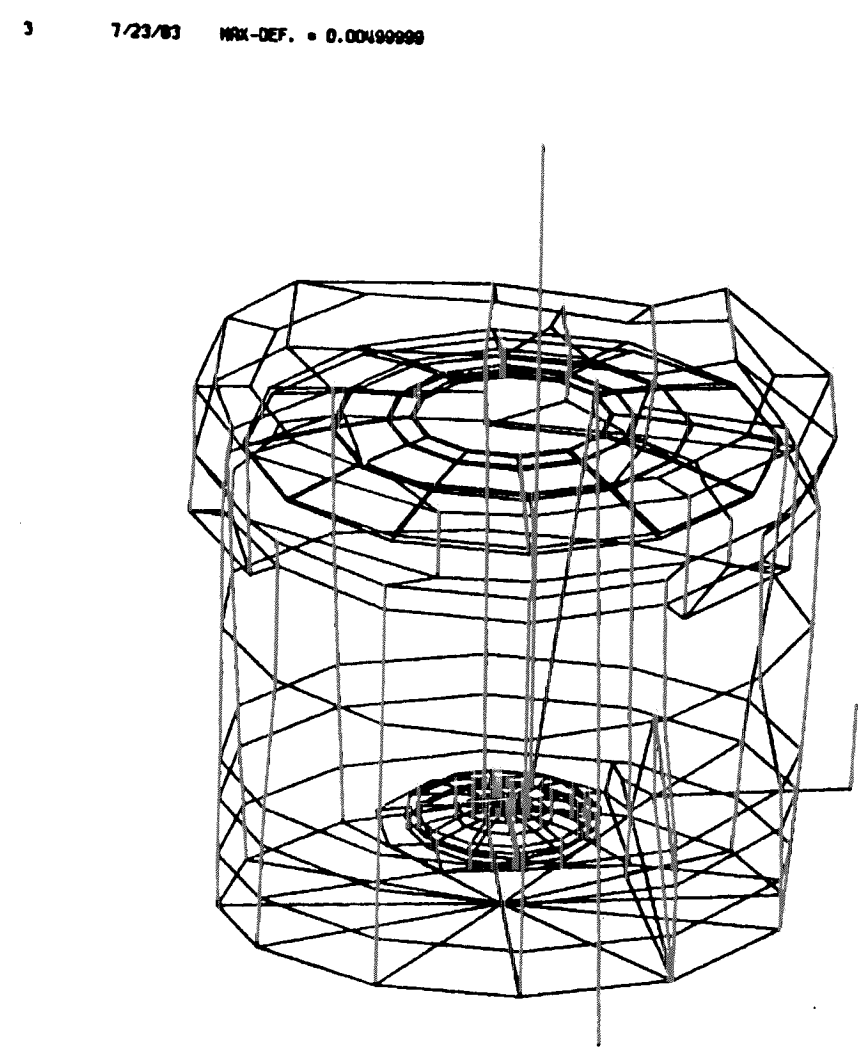

Figure 4. Telescope Deformed by Particle Under Flange.

SUBCASE 1

D I S P L A C E M E N T V E C T O R

POINT ID.	TYPE	T1	T2	T3	R1	R2	R3
1	G	0.0	0.0	0.0	0.0	0.0	0.0
2	G	0.0	0.0	0.0	0.0	0.0	0.0
3	G	0.0	0.0	0.0	0.0	0.0	0.0
10	G	0.0	0.0	0.0	0.0	0.0	0.0
130	G	1.780964E-03	-1.312758E-03	-4.029290E-04	-1.433174E-03	-2.024368E-05	6.870334E-05
131	G	1.870224E-03	-4.905306E-04	-4.018559E-04	-8.034213E-04	3.562615E-04	-1.231553E-03
132	G	1.376665E-03	-9.542242E-04	3.892416E-05	-8.379636E-05	-1.779259E-04	2.212846E-04
133	G	1.131981E-03	-9.444280E-04	3.701064E-05	-2.503538E-02	-5.447301E-02	3.026001E-04
134	G	1.451577E-03	-8.536513E-04	-1.436157E-04	1.434960E-04	2.073631E-04	-2.231054E-04
135	G	1.392994E-03	-9.505359E-04	-6.129745E-05	-2.506533E-05	-1.827456E-04	-1.885297E-04
140	G	1.372603E-03	-8.102199E-04	-1.390433E-04	-1.755088E-04	9.817882E-05	-5.437954E-05
141	G	1.382549E-03	-7.868596E-04	-7.067716E-05	-7.852876E-05	1.323877E-04	-1.682504E-05
142	G	1.378521E-03	-7.786747E-04	3.335016E-06	-7.345587E-05	1.169849E-04	0.0
143	G	1.363742E-03	-7.717214E-04	8.929584E-05	-4.764899E-05	9.335333E-05	0.0
144	G	1.351439E-03	-7.762794E-04	9.781375E-05	-4.402236E-05	7.922674E-05	0.0
145	G	1.346989E-03	-7.866360E-04	6.823879E-05	-4.267390E-05	6.670151E-05	0.0
146	G	1.348471E-03	-7.972881E-04	3.299252E-05	-4.270645E-05	3.514386E-05	-2.108095E-06
148	G	1.367170E-03	-8.077160E-04	-9.107207E-05	-1.430480E-04	9.037459E-05	-1.405858E-05
149	G	1.358949E-03	-8.003737E-04	-1.148280E-05	-8.864893E-05	6.209741E-05	-1.799185E-05
150	G	1.371181E-03	-7.986657E-04	-7.905231E-05	-1.382357E-04	9.594961E-05	-2.025437E-05
151	G	1.377672E-03	-7.846895E-04	-3.349791E-05	-8.241693E-05	1.239365E-04	-1.577400E-05
152	G	1.375664E-03	-7.807089E-04	1.546563E-06	-7.289767E-05	1.147566E-04	-1.922677E-05
153	G	1.365962E-03	-7.762412E-04	6.056904E-05	-5.715327E-05	9.709483E-05	-1.856682E-05
154	G	1.357058E-03	-7.778067E-04	7.820103E-05	-4.860528E-05	8.128127E-05	-1.849435E-05
155	G	1.352331E-03	-7.895832E-04	4.462610E-05	-4.656041E-05	6.015925E-05	-1.955085E-05
204	G	0.0	0.0	0.0	0.0	0.0	0.0
2000	G	0.0	0.0	0.0	0.0	0.0	0.0
2001	G	0.0	0.0	-7.391021E-05	-7.528844E-04	-8.230185E-04	0.0
2002	G	-2.825199E-04	2.568842E-04	7.027320E-04	3.866375E-04	-7.914720E-05	0.0
2003	G	2.132161E-04	2.190071E-03	0.0	-3.866375E-04	-9.914720E-05	0.0
10000	G	-3.661727E-05	2.219845E-04	1.395740E-04	-1.762552E-04	-4.510528E-04	-1.556958E-04
10001	G	2.152818E-05	2.377018E-04	2.881965E-05	-1.781570E-04	-4.514599E-04	-1.556078E-04
10002	G	6.399883E-05	2.804151E-04	-1.431575E-04	-1.818993E-04	-4.539497E-04	-1.610391E-04
10003	G	7.938245E-05	3.386432E-04	-3.305635E-04	-1.856071E-04	-4.572487E-04	-1.579587E-04
10004	G	6.358665E-05	3.967853E-04	-4.824096E-04	-1.874505E-04	-4.602087E-04	-1.519406E-04
10005	G	2.088067E-05	4.392367E-04	-5.571892E-04	-1.851154E-04	-4.620217E-04	-1.578048E-04
10006	G	-3.723452E-05	4.545681E-04	-5.352206E-04	-1.806139E-04	-4.603752E-04	-1.566679E-04
10007	G	-9.523664E-05	4.387435E-04	-4.232930E-04	-1.767797E-04	-4.569152E-04	-1.523766E-04
10008	G	-1.376259E-04	3.961073E-04	-2.518679E-04	-1.740632E-04	-4.534782E-04	-1.582924E-04
10009	G	-1.530515E-04	3.380812E-04	-6.629638E-05	-1.735187E-04	-4.522491E-04	-1.587382E-04
10010	G	-1.373855E-04	2.800143E-04	8.447000E-05	-1.739153E-04	-4.523351E-04	-1.548536E-04
10011	G	-9.478177E-05	2.374907E-04	1.599151E-04	-1.750460E-04	-4.516291E-04	-1.564820E-04
10100	G	-2.877383E-05	1.910850E-04	2.197072E-04	-1.765958E-04	-4.509825E-04	-1.578352E-04
10101	G	4.330295E-05	2.104760E-04	8.249020E-05	-1.780012E-04	-4.517795E-04	-1.568881E-04
10102	G	9.599342E-05	2.633217E-04	-1.307453E-04	-1.811929E-04	-4.544301E-04	-1.540877E-04
10103	G	1.151840E-04	3.353832E-04	-3.635355E-04	-1.855612E-04	-4.589130E-04	-1.605001E-04
10104	G	9.572492E-05	4.074203E-04	-5.521597E-04	-1.869824E-04	-4.618518E-04	-1.632945E-04
10105	G	4.284183E-05	4.600777E-04	-6.447154E-04	-1.863465E-04	-4.613988E-04	-1.525991E-04
10106	G	-2.918256E-05	4.791981E-04	-6.169999E-04	-1.822467E-04	-4.601984E-04	-1.527968E-04
10107	G	-1.011396E-04	4.597191E-04	-4.778258E-04	-1.771060E-04	-4.561994E-04	-1.592578E-04

Figure 5. Boresight Loss Caused by Particle.

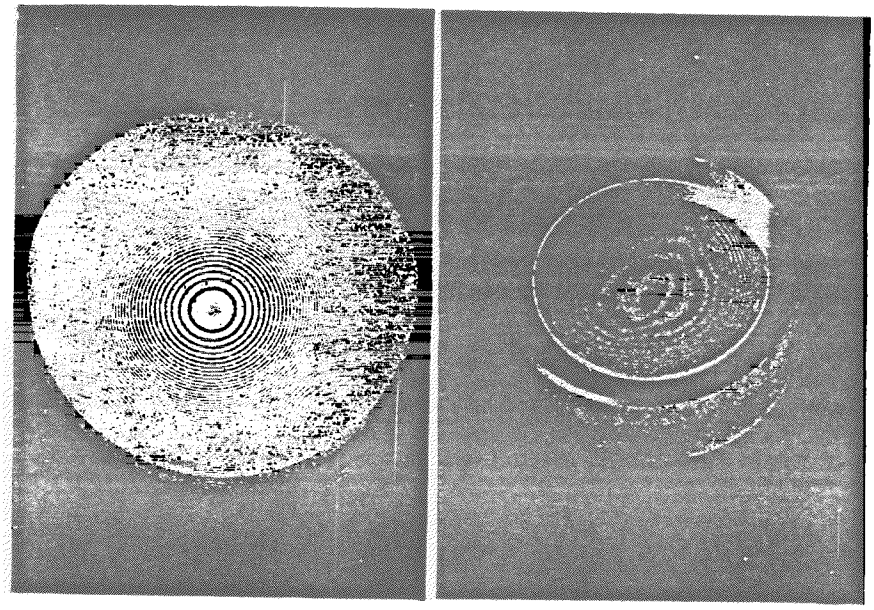

Figure 6. Interferance Fringes.

(a) Newton's Rings between a convex and a place surface.
(b) Fringe pattern of a telescope objective under test.
(From Sears and Zemansky, University Physics, 1949)

7 7/23/83 MAX-DEF. = 0.00499999
X. BOLT LOCATIONS

7

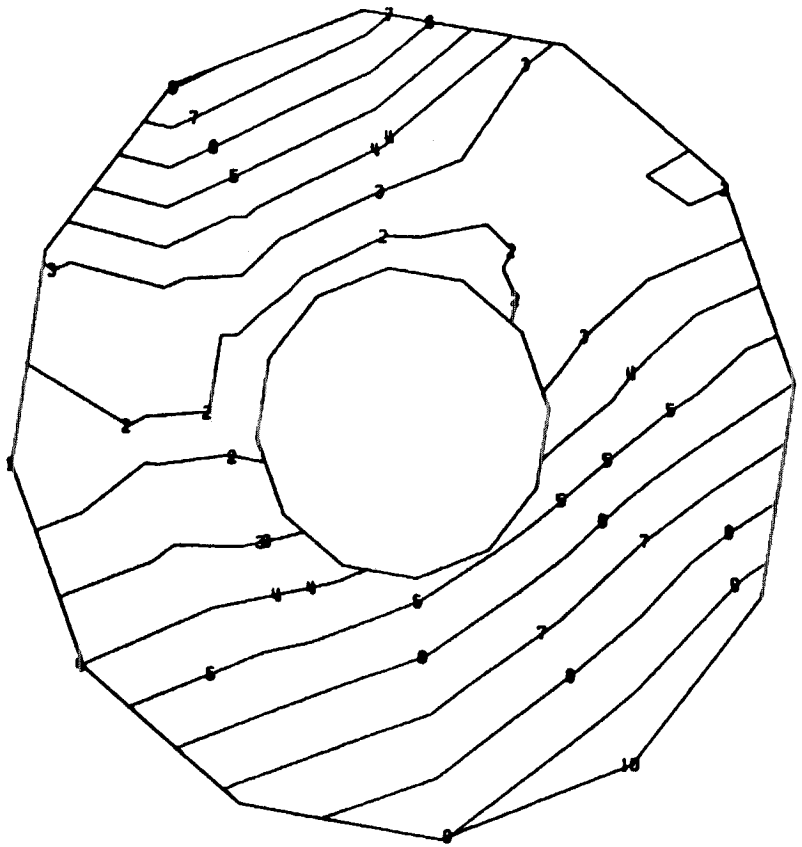

7

SYMBOL	VALUE (INCHES)
1	-1.21E-05
2	-1.01E-05
3	-8.18E-06
4	-6.21E-06
5	-4.24E-06
6	-2.27E-06
7	-2.99E-07
8	1.67E-06
9	3.64E-06
10	5.61E-06

TOTAL RANGE:

INCHES	1.77E-05
NM	450
WAVES,HeNe	.71
FRINGES,"	1.42

OPTICAL TELESCOPE
.005 PARTICLE AT 70100 GRID.
STATIC DEFOR. SUBCASE 1 LOAD 300

Figure 7. Primary Mirror, Ten Equal Contours, Particle in Flange.

15 7/23/93 MAX-DEF. = 0.00499998
X. BOLT LOCATIONS.

15

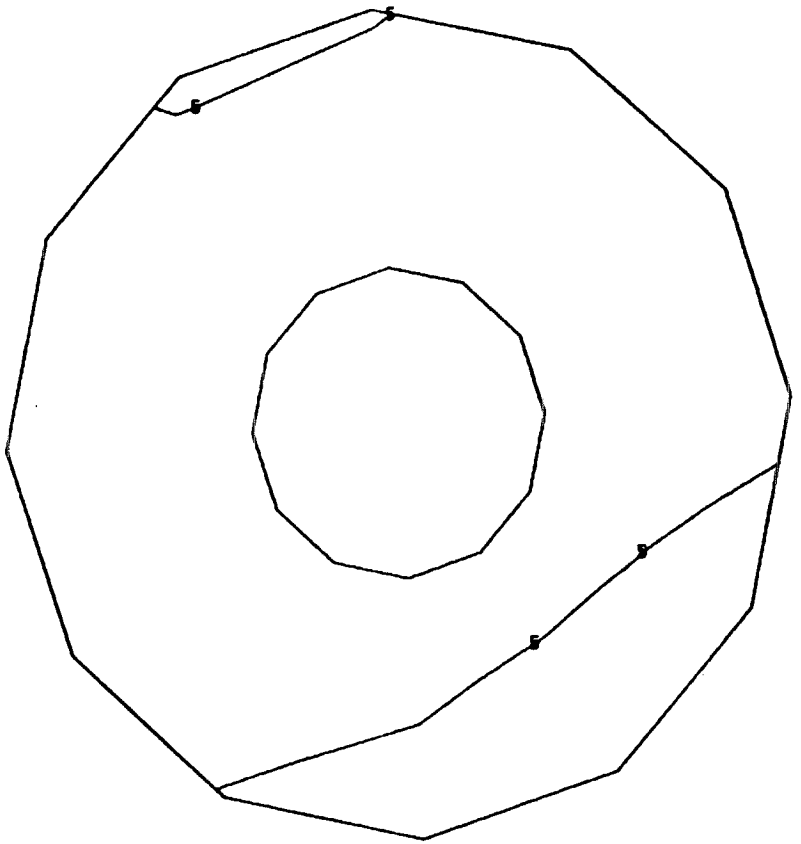

15

SYMBOL	VALUE (INCHES)	SYMBOL	VALUE (INCHES)
1	5.00E-05	15	-1.25E-04
2	3.75E-05	16	-1.38E-04
3	2.50E-05	17	-1.50E-04
4	1.25E-05	18	-1.62E-04
5	0.0	19	-1.75E-04
6	-1.25E-05	20	-1.88E-04
7	-2.50E-05	21	-2.00E-04
8	-3.75E-05	22	-2.12E-04
9	-5.00E-05	23	-2.25E-04
10	-6.25E-05	24	-2.38E-04
11	-7.50E-05	25	-2.50E-04
12	-8.75E-05	26	-2.62E-04
13	-1.00E-04	27	-2.75E-04
14	-1.12E-04		

EACH CONTOUR REPRESENTS:
12.5 microinches (317 nanometers) change in figure,
Half a wavelength in HeNe laser light, and
The center of a dark band under a test plate
illuminated with HeNe light.

OPTICAL TELESCOPE
.005 PARTICLE AT 70100 GRID.
STATIC DEFOR. SUBCASE 1 LOAD 300

Figure 8. Primary Mirror, HeNe Illumination, Particle in Flange.

16 7/23/83 MAX-DEF. = 0.08750724
X. SCALE LOCATIONS.

16

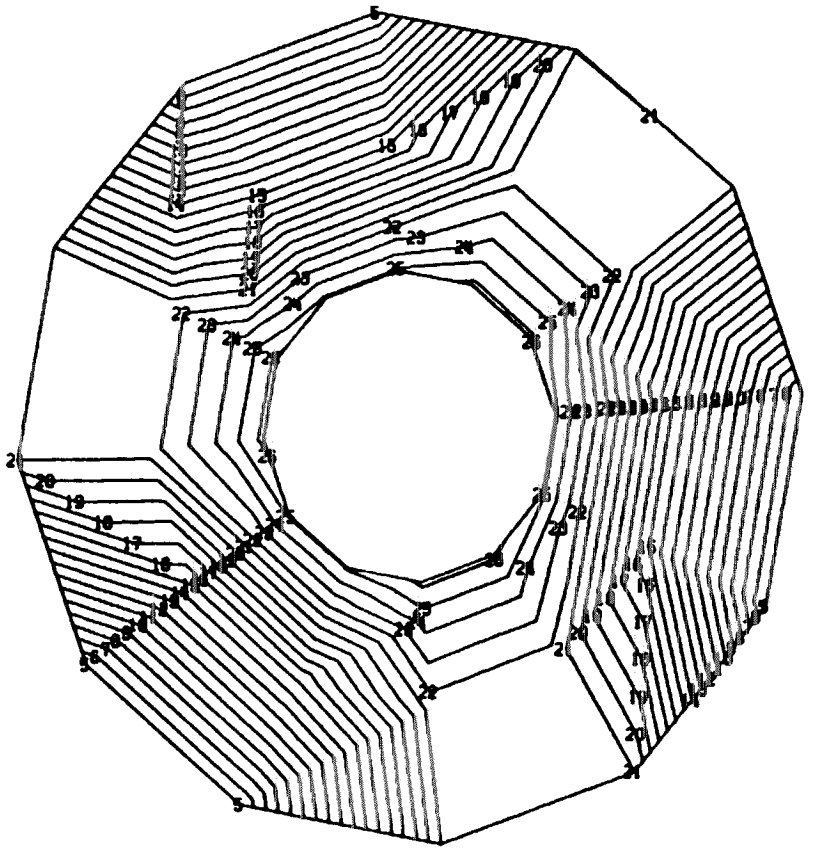

SYMBOL	VALUE (INCHES)	SYMBOL	VALUE (INCHES)
1	5.00E-05	15	-1.25E-04
2	3.75E-05	16	-1.38E-04
3	2.50E-05	17	-1.50E-04
4	1.25E-05	18	-1.62E-04
5	0.0	19	-1.75E-04
6	-1.25E-05	20	-1.88E-04
7	-2.50E-05	21	-2.00E-04
8	-3.75E-05	22	-2.12E-04
9	-5.00E-05	23	-2.25E-04
10	-6.25E-05	24	-2.38E-04
11	-7.50E-05	25	-2.50E-04
12	-8.75E-05	26	-2.62E-04
13	-1.00E-04	27	-2.75E-04
14	-1.12E-04		

EACH CONTOUR REPRESENTS:
12.5 microinches (317 nanometers) change in figure,
Half a wavelength in HeNe laser light, and
The center of a dark band under a test plate
illuminated with HeNe light.

AEOCAL TELESCOPE
100 G AXIAL ACCELERATION.
STATIC DEFOR. SUBCASE 2 LOAD 400

Figure 9. Primary Mirror, HeNe Illumination, 100 gs accel.